Influence of yeast size on the kinetics of cell disruption in an ultrasonic homogenizer

Anna Kacprowicz [ID], Marek Solecki* [ID]

Lodz University of Technology, Faculty of Process and Environmental Engineering, Wolczanska 213, 93-005 Lodz, Poland

* **Corresponding author, e-mail:**
marek.solecki@p.lodz.pl

Abstract

The results of studies on the disintegration kinetics of the yeast *Saccharomyces cerevisiae* are presented. The process was carried out in a 500 W ultrasonic homogenizer equipped with a spherical working chamber with a volume of 100 cm^3. The concentration of the suspension of microorganisms was 0.05 g d.m./cm^3. The continuous phase was water solution containing 0.15 M NaCl and 4 mM K$_2$HPO$_4$. The kinetics of cell disruption were studied by the direct method. The theory of random transformation of dispersed matter was used to analyze the process. There was significant variation in the size of yeast cells. The range of changes in the values of parameters describing the size of microorganisms was divided into size classes. The kinetics of cell disruption in individual classes was described by a first-order linear differential equation. During the implosion of cavitation bubbles, the transformation volume of individual microorganisms is generated. It has been shown that as the volume of cells in subsequent size classes increases, their transformation volumes do not increase significantly. The safe volume for cells remains unchanged. As the size of the microorganisms increased, there was no increase in the constant rate of cell disruption.

Keywords

microorganisms, disintegration process, ultrasounds, process kinetics

1. INTRODUCTION

Many compounds contained inside microbial cells have found commercial use in the food, chemical and pharmaceutical industries, as well as medicine, agriculture and environmental protection. In order to isolate these compounds, it is generally necessary to disrupt the cell walls and cytoplasmic membranes of microorganisms. High-pressure homogenizers and bead mills are used to carry out this process on an industrial scale (Chisti and Moo-Young, 1986; Geciova et al., 2002). For many years, research has been carried out on improving the process of microorganism disintegration during ultrasonic cavitation (Borthwick et al., 2005; Doulah, 1977; Dumitrașcu et al., 2022; Nogueira et al., 2018; Patil et al., 2018; Weber et al., 2022; Yusaf, 2015; Zheng et al., 2021). Despite many advantages, such as simple structure, small size, easy operation, easy sterilization, ability to work in a continuous (flow) system, devices implementing the process using this method are generally not used industrially (Chisti and Moo-Young, 1986; Geciova et al., 2002). The exception is the use of the ultrasonic method for disintegration of sewage sludge (Chu et al., 2000; Zielewicz, 2016). The reason for this condition is usually the lack of satisfactory efficiency of the process carried out in ultrasonic homogenizers. In the case of devices used on a laboratory scale, this deficiency is insignificant compared to the advantages.

To improve processes carried out in bead mills, a methodology has been developed that allows building a phenomenological model and making a mathematical description based on it.

Based on the results obtained from research on the disintegration of microorganisms, a general theory of processes involving random transformation of dispersed matter was formulated (Solecki, 2011; 2013). It allows for systematizing and rationalizing ontological facts, explaining the causes of their occurrence, predicting events, modifying existing and building new devices. The developed theory was used to study the influence of the size of microorganisms on the cell disruption process in a bead mill (Solecki et al., 2021). It seems that the process of disintegration of microorganisms in ultrasonic homogenizers is also a random transformation process and the developed theory can be used to analyze it.

The aim of the work was to investigate the possibility of using the theory of random transformation of dispersed matter to describe the process of ultrasonic disintegration of microbial cells. Considerations on the process were carried out for two different variants of the assumed characteristics of the transformed objects: homogeneity and heterogeneity of microorganisms belonging to the set N.

2. MATERIAL AND METHODS

2.1. Biological material

The biological material used to study the disintegration process of microbial cells was commercial baker's yeast, *Saccharomyces cerevisiae*. They were manufactured by Lesaffre Polska S.A. in Wołczyn. All experiments were performed using

yeast from a single fermentation. They were used no longer than 21 days from the date of production. During this period, there was no effect of storage time on the susceptibility of cells to disintegration. ultrasonic. The material formed in the form of cubes weighing 500 g was stored at a temperature of 4 °C.

The experiments were carried out for a yeast suspension with a concentration of 0.05 g d.w./cm^3±5%. Its continuous phase was an aqueous solution containing 0.15 M NaCl and 4 mM K$_2$HPO$_4$.

2.2. Research device

Disintegration of yeast cells was carried out in an ultrasonic homogenizer shown in Fig. 1. It consisted of an ultrasonic processor VCX-500 Vibra Cell Ultra Sonic Processor (Sonics & Materials Inc.) with a power of 500 W. The 24 kHz sound generator was connected to a converter equipped with a titanium alloy tip with a diameter of 13 mm. Its rated vibration amplitude was 114 μm.
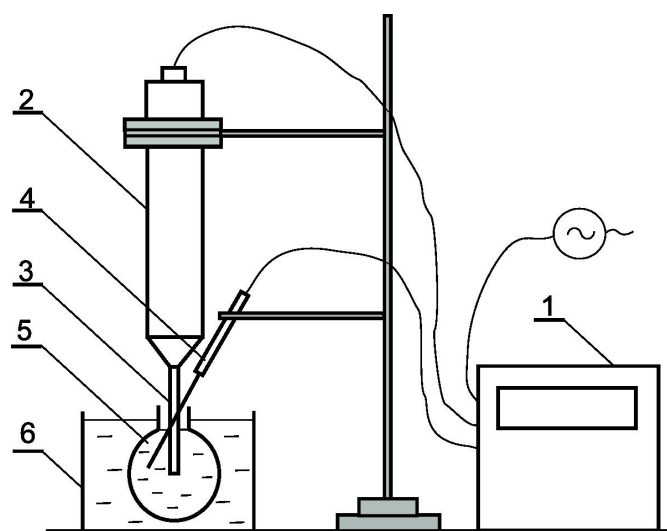

Figure 1. Diagram of the research stand for ultrasonic disintegration of microbial cells, 1 – ultrasound generator, 2 – converter, 3 – tip, 4 – thermocouple, 5 – working chamber, 6 – water bath.

The suspension of microorganisms was placed in a working chamber with a spherical shape and a volume of 100 cm^3 (Kacprowicz et al., 2020). The experiments were performed for constant batch (periodic operation). During the process, the vibration amplitude of the tip located in the center of the working chamber sphere was 40% of the rated amplitude. The cyclic active time was 0.6 s and the inactive time was 0.3 s. The released heat was removed by placing the working chamber in a water bath cooled with ice in the presence of NaCl. The temperature of the suspension during the process varied from 4 to 10 °C. The disintegration process was carried out from $t_0 = 0$ s to $t_k = 6000$ s, suspension samples with a volume of 3 cm^3 were taken every 1200 s.

2.3. Methodology and results preparation

During the process of ultrasonic disintegration of yeast, the kinetics of microbial cell disruption and the kinetics of the release of intracellular compounds were examined. The course of the process of transformation of objects from the N set as a result of disrupting the cell walls of microorganisms was examined by the direct method. The number of dead cells in subsequent suspension samples was determined based on the number of live cells N in relation to the number of live cells present in the zero sample N_0. The degree of yeast cell disruption was determined according to Eq. (1).

$$X_1 = \frac{N_0 - N}{N_0} 100\% \qquad (1)$$

Computer analysis of microscopic images was used to study living microorganisms. The collected samples were diluted 10, 20 and 50 times depending on the concentration of living cells. An Olympus BX51 research microscope (Olympus Optical CO., Ltd) equipped with an XC 50 digital camera (Olympus Soft Imiging Solutions GmbH) was used. A Thoma neu chamber (Paul Marienfeld GmbH & Co.) was used to count the cells present in the suspension samples. The obtained microscopic images were analyzed using analySIS 5 software (Soft Imaging System GmbH). 24-bit RGB images were transformed into 8-bit grayscale images (256 shades). The initial and final stages of photo processing are shown in Fig. 2.

The few characteristic chains of cells created by yeast were "cut" in the photos so that separate cells were isolated during detection. "Cutting" involved drawing a line dividing contacting cells. The line was definitely brighter than the selected threshold for automatic detection of microorganisms and had the smallest possible width to effectively separate the contacting objects. Solecki et al. (2013) showed no significant impact of such a treatment on the values of determined parameters describing microbial cells.

The few budding yeasts, which constituted 0.89% of the population, were omitted from the considerations. For the sensitivity threshold established on the basis of all images, objects belonging to the N set were automatically detected. Accidental contamination was eliminated using morphological filters built into the program. Selected parameters such as D_{min}, D_{mean}, D_{max}, *Elongation* were automatically measured. Their values were determined on the basis of measurements passing through the center of the cell, taken from the outer edge to the outer edge in the range from 0 to 179° in 1o increments: The few budding yeasts, which constituted 0.89% of the population, were omitted from the considerations. For the sensitivity threshold established on the basis of all images, objects belonging to the N set were automatically detected. Accidental contamination was eliminated using morphological filters built into the program. Selected parameters such as D_{min}, D_{mean}, D_{max}, *Elongation* were automatically measured.
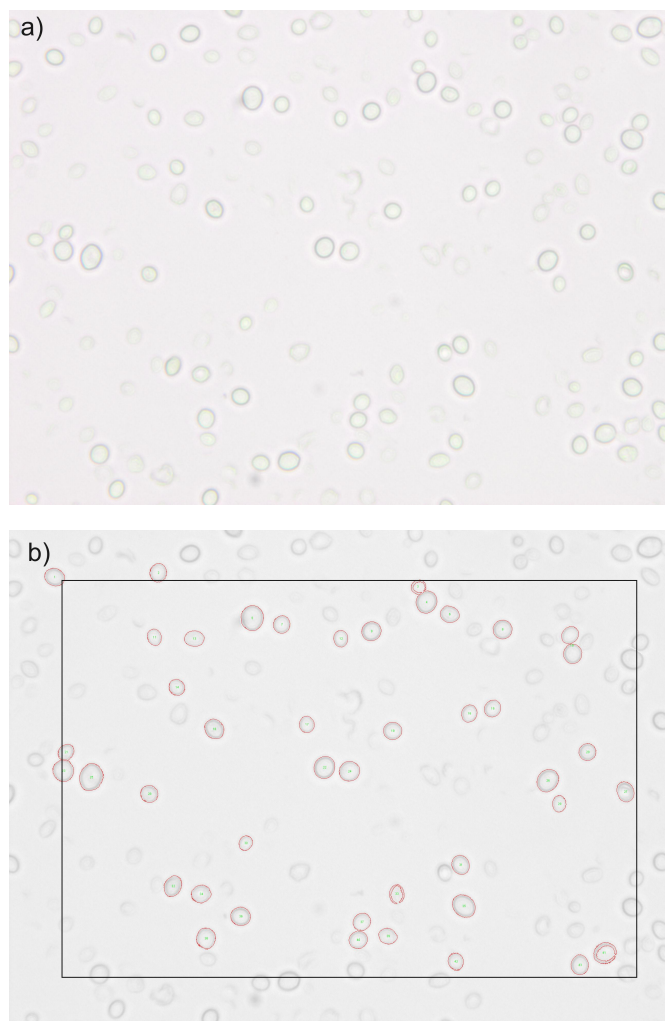
Figure 2. Stages of processing microscopic images of *S. cerevisiae* yeast cells subjected to disintegration in an ultrasonic homogenizer (process duration $t = 2400$ s, lens magnification $40\times$, dilution $r = 25\times$): a) initial photo – TIFF 24 bit RGB, b) photo after detection of live cells – TIFF 8 bit grayscale (rectangular area – measurements of detected objects, red highlight – cells identified as alive).

Their values were determined on the basis of measurements passing through the center of the cell, taken from the outer edge to the outer edge in the range from 0 to $179°$ in $1°$ increments:

D_{mean} – arithmetic mean of all (180) measurements;
D_{min} – the smallest cell measurement;
D_{max} – the largest cell measurement;
Elongation – the squared quotient of the longitudinal value and the transverse deviation of all pixels belonging to the object determined along the regression line.

The obtained results of automatic detection were visually verified for all photos taken for the sample taken after the process duration of 0 s. The obtained parameter limit values were used to perform additional morphological filters eliminating from the N set objects with an appearance similar to living

yeast cells.

The kinetics of the release of intracellular compounds were determined based on the analysis of the amount of released nucleic acids. It was determined using the spectrophotometric method by measuring absorbance at a wavelength of $\lambda = 260$ nm (Heim and Solecki, 1999; Kacprowicz et al., 2020; Middelberg et al., 1991). The maxima of nucleic acid spectra occur near this length. The supernatant was obtained after 20 minutes of centrifugation at a centrifugal force of 34,000 g, and measurements were made on a Lambda 11 spectrophotometer (Perkin Elmer). The obtained absorbance values A at a given dilution r of samples were converted to the concentration C of pure RNA nucleic acid (Eq. (2)) (Benthin et al., 1991).

$$C = M \frac{Ar - A_0 r_0}{\varepsilon l} \tag{2}$$

The degree of nucleic acid release was determined according to Eq. (3).

$$X_2 = \frac{C}{C_{\text{max}}} 100\% \tag{3}$$

The maximum amount of C_{max} nucleic acids that could be released was determined experimentally after a long-term disintegration process ($X_2 > 90\%$), assuming the linearity of the process.

3. RESULTS AND DISCUSSION

When carrying out the process of disintegration of microorganisms in an ultrasonic homogenizer, yeast cells suspended in the continuous phase constitute dispersed material objects of the N set. The suspension occupies volume V, in which intense mixing takes place to homogenize the yeast concentration. The volume of individual microorganisms is incomparably smaller than V. In volume V, transformation volumes $V_{\gamma i}$ are randomly generated, also much smaller than volume V. A cell introduced into volume $V_{\gamma i}$ is transformed due to the physical conditions prevailing in it. It involves depriving a cell of at least one important feature that determines its membership in set N. The conditions and course of the process of disintegration of microorganism cells in an ultrasonic homogenizer meet all the assumptions adopted in the theory of random transformation of dispersed matter (Solecki, 2013). The processes carried out in the pearl mill and ultrasonic homogenizer differ in the way they produce volumes $V_{\gamma i}$ and $V_{\beta i}$. The volume $V_{\beta i}$ is inaccessible to living microbial cells. In the case of a mill, they are produced by the surfaces of two solids. One is the surface of the ball filling the mill, the other is the surface of the adjacent ball, mixer or working tank (Solecki, 2011; 2013). In an ultrasonic homogenizer, $V_{\gamma i}$ and $V_{\beta i}$ are produced as a result of the impact of the liquid surface during the implosion of gas bubbles or as a result of the large liquid velocity gradient resulting from the vortices generated during the implosion.

The kinetics of the yeast disruption process, assuming cell homogeneity, are described by Eq. (4).

$$dN_d = k_1 (N_0 - N_d) \, dt \tag{4}$$

After separating the variables and integrating both sides of Eq. (4), Eq. (5) was obtained.

$$\ln \left(\frac{N_0}{N_0 - N_d} \right) = k_1 t \tag{5}$$

The designation consistent with Eq. (6) was adopted.

$$B_1 = \frac{N_0}{N_0 - N_d} \tag{6}$$

The kinetics of the cell disruption process were determined by describing the experimental data with a regression line consistent with Eq. (5). The obtained results are graphically presented in Fig. 2. The determined value of the cell bursting rate constant k_1 was 0.0005270 s^{-1} and its standard error was 7.915x10^{-5}. The determined value of the R^2 coefficient was equal to 0.8986.

The kinetics of nucleic acid release from inside yeast cells is described by Eq. (7).

$$\frac{dC}{dt} = k_2 (C_{\max} - C) \tag{7}$$

After simple mathematical transformations of Eq. (7), Eq. (8) was obtained.

$$\ln \frac{C_{\max}}{C_{\max} - C} = k_2 t \tag{8}$$

The designation adopted is consistent with Eq. (9).

$$B_2 = \frac{C_{\max}}{C_{\max} - C} \tag{9}$$

A comparison of changes in the degree of yeast cell disruption and the degree of nucleic acid release is shown in Fig. 3. The kinetics of the nucleic acid release process were determined by describing the experimental data with a regression line, equation (8). The obtained results are graphically presented in Fig. 4. The determined value of the nucleic acid release rate constant, k_2, was 0.0004658 s^{-1} and its standard error was $1.145 \cdot 10^{-5}$. The R^2 coefficient was equal to 0.9970.

The obtained course of the cell disruption process and the nucleic acid release process (Fig. 4) show that the rate constant k_1 is slightly larger than the constant k_2. First, the cells are disrupted, then the intracellular compounds are released and dissolved in the continuous phase. Hence, the rate of yeast disruption is greater than the rate of release of intracellular compounds. The differences between the constants are not large, about 10%.

The results of morphological tests show significant differences in the cell sizes of the microorganisms used. The extreme values of the measured parameters are summarized in Table 1.
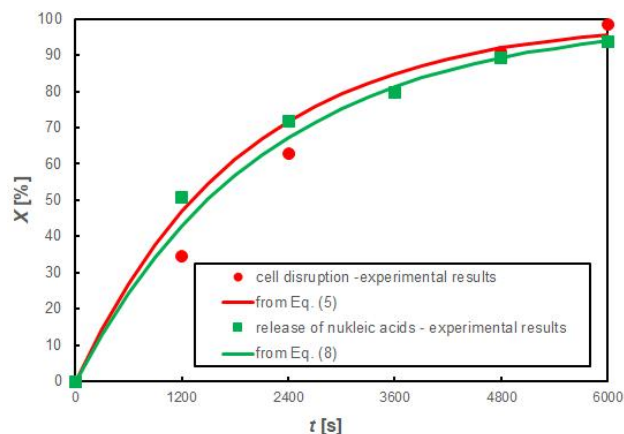

Figure 3. Changes in the degree of disruption of yeast cells and the release of nucleic acids from them during ultrasonic disintegration.
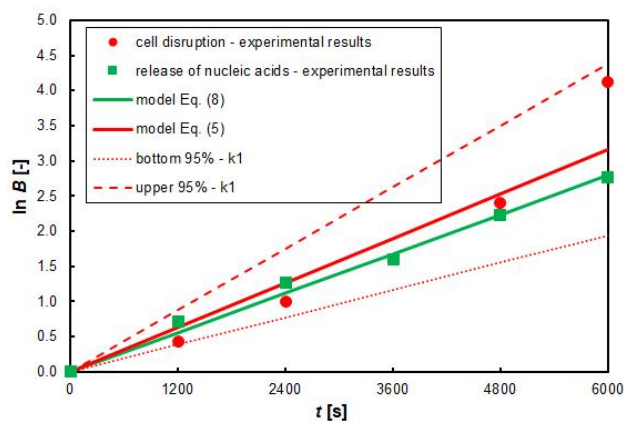

Figure 4. The process of disrupting yeast cells and releasing nucleic acids from them during ultrasonic disintegration.

Table 1. Limit values of yeast geometric parameters.

	$D_{\min}$	D_{mean}	$D_{\max}$	Elongation
	μm	μm	μm	–
Minimal	2.77	2.93	3.09	1.00
Maximal	7.34	8.54	8.70	1.50

The D_{mean} parameter, used to describe the shape of cells with a spherical model, increases by 65%. In turn, the $D_{\min}$ and $D_{\max}$ parameters, used in the ellipsoidal description of the cell shape, increase their values by approximately 1.8 times. The values of the Elongation parameter indicate that the set of material objects N includes cells with a shape close to spherical and close to ellipsoidal, with significant differences in flattening. In order to investigate the influence of the size of yeast cells on the process of their ultrasonic disintegration, the set of material objects was divided into size classes. Based on the number of N_0 objects belonging to the set N, the number of size classes was determined from Eq. (10).

$$m \approx 1 + 3.322 \log (N_0) \tag{10}$$

The distribution series was determined on the basis of the ranges of the $D_{\min}$, D_{mean} and $D_{\max}$ parameters presented in Table 1 and the division of $N_0 = 1056$ objects into 11 size classes. The obtained effects were used to analyze the distribution of average sizes of diameters $\overline{D_{\text{mean}}}$, $\overline{D_{\min}}$ and $\overline{D_{\max}}$ describing microbial cells in Figs. 5, 6 and 7.
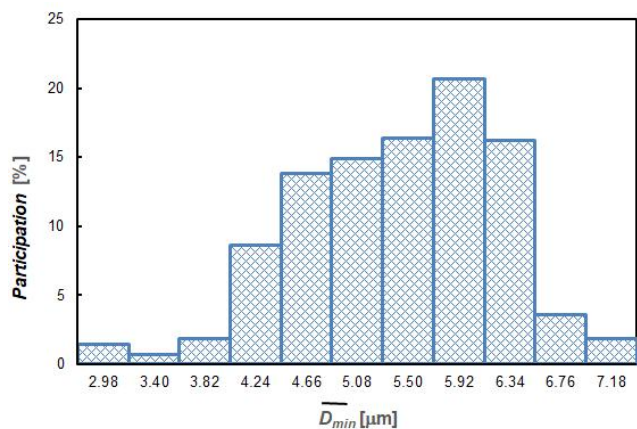

Figure 5. Cell size distribution depending on the size class described by the average diameter value D_{mean} (process duration $t = 0$ s).
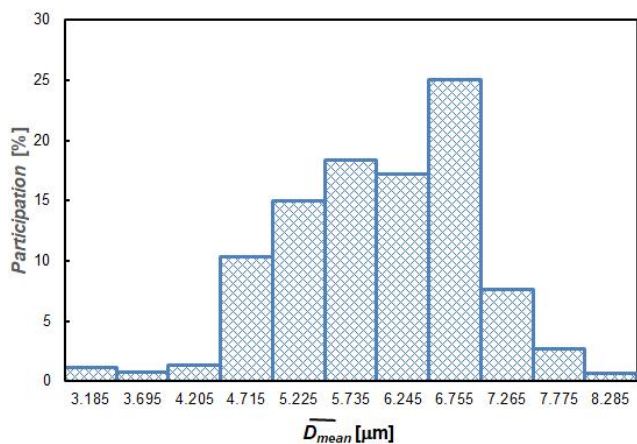

Figure 6. Cell size distribution depending on the size class described by the average diameter value $D_{\min}$ (process duration $t = 0$ s).

We assume that material objects belonging to the set N differ in only one feature that has a significant impact on the process. In the case of modeling the shape of yeast cells with a spherical surface, the parameter describing individual objects will be the diameter D_{mean}. The entire domain of this parameter was divided into m intervals (Fig. 5). The process of transforming objects from any range ζ, where

$$\zeta \epsilon < \langle 1; m \rangle \tag{11}$$

is described by Eq. (12) taking into account the existence of the entire set N (Solecki, 2013; Solecki et al. 2021).

$$\frac{N_{o\zeta}}{N_0} \mathrm{d}N_{d\zeta} = \frac{N_0}{N_0} k_{1\zeta} \left(N_{0\zeta} - N_{d\zeta} \right) \mathrm{d}t \tag{12}$$
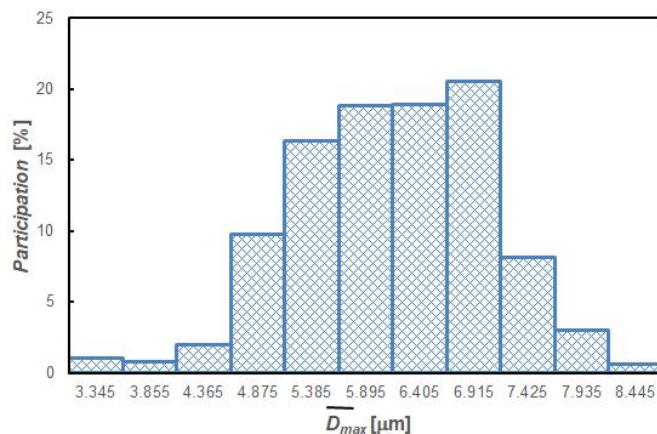

Figure 7. Cell size distribution depending on the size class described by the average diameter value $D_{\max}$ (process duration $t = 0$ s).

After simple mathematical transformations of Eq. (12), we obtain Eq. (13).

$$\frac{N_{0\zeta}}{N_0} \ln \frac{N_{0\zeta}}{N_{0\zeta} - N_{d\zeta}} = \frac{N_{0\zeta}}{N_0} k_{1\zeta} t \tag{13}$$

Eq. (13) was used to describe the course of the yeast cell disruption process in individual size classes. The designation adopted is consistent with Eq. (14).

$$B_{1\zeta} = \frac{N_{0\zeta}}{N_{0\zeta} - N_{d\zeta}} \tag{14}$$

A comparison of changes in X_1 parameters during the disintegration of yeast cells for selected size classes is shown in Fig. 8. During the selection process, the two lowest and two highest size classes were rejected due to large measurement errors resulting from the small number of cells in these classes. Three classes were selected from the remaining classes, spaced every 3 classes. The course of the cell disruption process in size classes is described by linear relationships (13) (Fig. 9). The obtained R^2 values for individual classes ranged from 0.9916 to 0.8379. In general, lower R^2 values were obtained for the extreme size classes in which the number of cells is the smallest (Fig. 5). The size of the measurement errors of experimental parameters depends on the number of cells counted.

If the ellipsoidal model is adopted, the cells can be described by diameters $D_{\min}$ and $D_{\max}$, with the simplifying assumption that the two shorter axes are equal. The ranges of these parameters have also been divided into 11 size classes. The kinetics in individual classes are described by a first-order linear differential equation. The results obtained are similar to those obtained for D_{mean} (Fig. 9). The R^2 parameter values for $D_{\min}$ and $D_{\max}$ range from 0.9876 to 0.8439 and from 0.9894 to 0.8439, respectively. The exception is class 11, where for $\overline{D_{\max}} = 9.045$ μm R^2 is 0.7448.

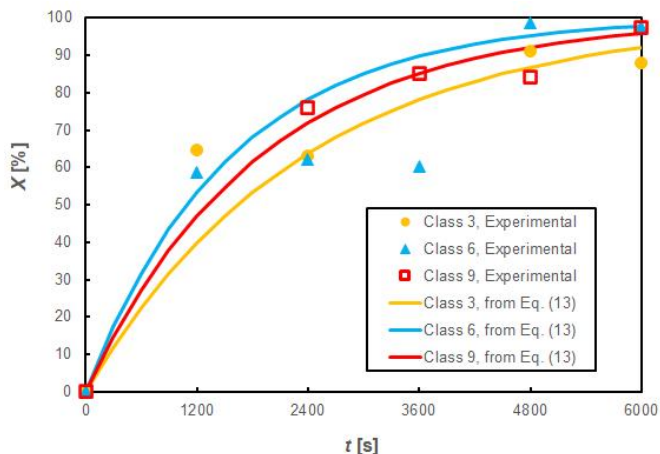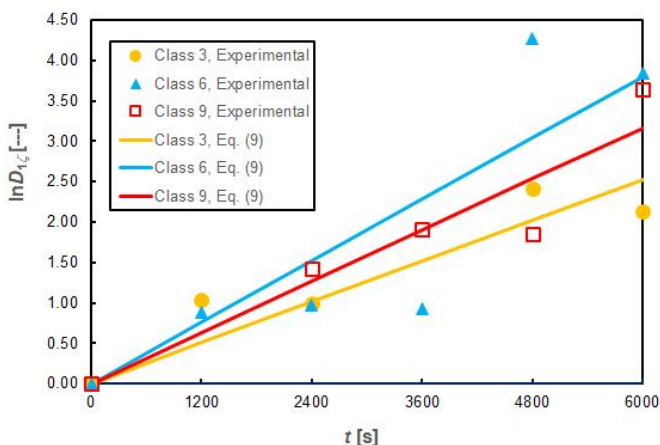Figure 8. Changes in the degree of yeast cell disruption during the process for selected cell size classes described by the D_{mean} parameter.

Figure 9. The course of yeast cell disruption in selected cell size classes described by the D_{mean} parameter.

The relationship between the process rate constants k_1 and $k_{1\zeta}$ in Eqs (4) and (12) is determined by Eq. (15) (Solecki, 2013).

$$\Phi \sum_{\zeta=1}^{m} \frac{N_{0\zeta}}{N_0} k_{1\zeta} = k_1. \tag{15}$$

The Φ coefficient is described by Eq. (16).

$$\Phi = \frac{\ln \dfrac{N_0}{N_0 - N_d}}{\displaystyle\sum_{\zeta=1}^{m} \frac{N_{0\zeta}}{N_0} \ln \frac{N_{0\zeta}}{N_{0\zeta} - N_{d\zeta}}}. \tag{16}$$

In the case of independent events, equation (15) shows that if partial processes are linear, their total course will also be linear.

The relationships between $k_{1\zeta}$ and the diameter $\overline{D_{\text{min}}}$, $\overline{D_{\text{mean}}}$ and $\overline{D_{\text{max}}}$ are shown in Fig. 10, 11 and 12, respectively. Based on the results obtained, it may seem that with increasing

the size class there is a slight increase in the constant rate $k_{1\zeta}$. It may reach approximately 30%. This result may be similar to that obtained for the disintegration process carried out in a pearl mill, but its effect of increasing the rate of cell disruption would be much smaller. During the disintegration of yeast cells in a bead mill with an increase in D_{mean} from the lowest to the highest value, the cell disruption rate constant increased approximately 10 times (Solecki, 2013).

The expected result of the process carried out in the ultrasonic homogenizer was a slight increase in the constant rate of cell disruption in the classes. The rate constant k_1 from Eq. (4) is described by Eq. (17) (Solecki, 2013).

$$k_1 = \frac{Fu}{V_\alpha} \tag{17}$$
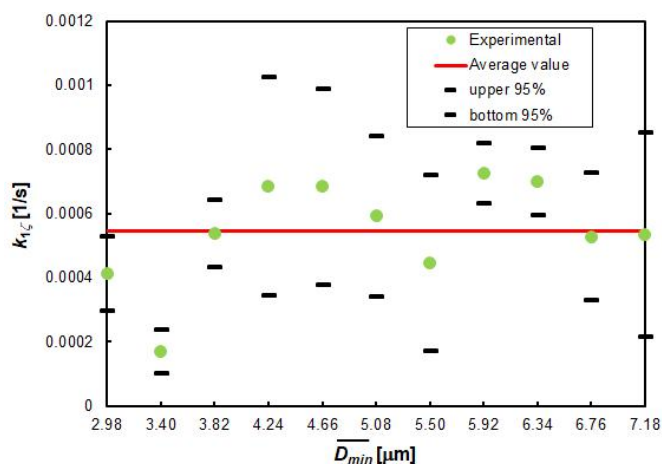

Figure 10. The influence of the cell size described by the average diameter value D_{min} on the rate constant of the yeast cell disruption process $k_{1\zeta}$ in an ultrasonic homogenizer.
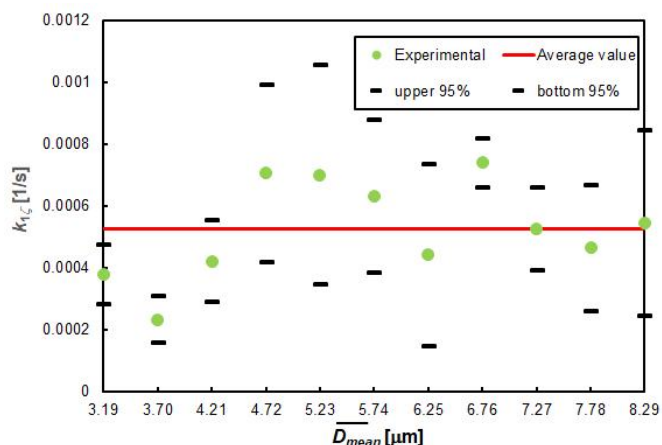

Figure 11. The influence of the cell size described by the average diameter value D_{mean} on the rate constant of the yeast cell disruption process $k_{1\zeta}$ in an ultrasonic homogenizer.
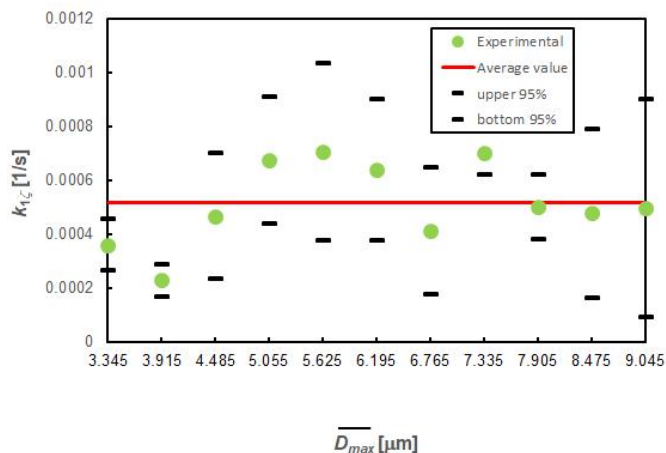
Figure 12. The influence of the cell size described by the average diameter value D_{max} on the rate constant of the yeast cell disruption process $k_{1\zeta}$ in an ultrasonic homogenizer.

The volume occupied by the suspension is given by Eq. (18).

$$V = V_\alpha + V_\beta \tag{18}$$

The rate constant $k_{1\zeta}$ from Eq. (12) is described by Eq. (19) (Solecki, 2013).

$$k_{1\zeta} = \frac{F_\zeta u_\zeta}{V_{\alpha\zeta}} \tag{19}$$

For cells of class $\zeta-$th microorganisms, the division of the suspension volume is described by Eq. (20).

$$V = V_{\alpha\zeta} + V_{\beta\zeta} \tag{20}$$

In a bead mill, when the cell is torn apart non axially between two colliding beads, the transformation volumes $V_{\gamma i}$ produced are many times larger than the volume of the destroyed cell of the ζ-th size class (Solecki, 2011; 2013). The size of $V_{\gamma\zeta}$ depends on the size of microorganisms from class z and on the distance of the event (cell disruption) from the axis of impact of the beads.

The volumes inaccessible to a living cell from the ζ-th class are even larger. The volume $V_{\gamma\zeta}$ is only a fraction of the volume $V_{\beta\zeta}$. If the volume $V_{\beta\zeta}$ increases in subsequent higher size classes, the safe volume for $V_{\alpha\zeta}$ cells decreases more and more (Eq. 21). According to Eq. (19), this effect causes an increase in the process speed constant.

Presumably, in an ultrasonic homogenizer, cells are disrupted by the implosion of adhering gas bubbles. The cells are deformed as a result of the impact of the liquid surface moving at a speed comparable to the speed of sound in the continuous phase of suspension. On the one hand, the cell wall is affected by normal stresses resulting from the impact of the liquid surface, and on the other hand, by internal pressure that increases during deformation. It appears that wall disruption occurs when critical stresses in the microbial coating are exceeded at

the point of cell impact. Cavitation bubbles are smaller than microorganisms. The transformation volumes $V_{\gamma\zeta}$ for a cell from the ζ-th size class arise only during the implosion of gas bubbles and is equal to the cell size. The volumes $V_{\gamma\zeta}$ are equal to the volume $V_{\beta\zeta}$, which is many times smaller than that produced in the mill (during non-axial impact of the balls). The rate constant $k_{1\zeta}$ is the larger the smaller the volume safe for microorganisms $V_{\alpha\zeta}$ is (Eq. (19)). This, in turn, is the smaller the larger the volume $V_{\beta\zeta}$ (Eq. (20)). Generally, the rate constant $k_{1\zeta}$ obtained in a bead mill is approximately 10 times higher than that obtained in an ultrasonic disintegrator.

The relationship between $k_{1\zeta}$ and the diameter $\overline{D_{\text{min}}}$, $\overline{D_{\text{mean}}}$ and $\overline{D_{\text{max}}}$ (Figs. 7, 8 and 9) is described by Eq. (21), (22) and (23).

$$k_{1\zeta} = b\overline{D_{\text{min}}} + a \tag{21}$$

$$k_{1\zeta} = b\overline{D_{\text{mean}}} + a \tag{22}$$

$$k_{1\zeta} = b\overline{D_{\text{max}}} + a \tag{23}$$

The results of multiple regression obtained using the STATISTICA PL program are presented in Table 2. The obtained results of the linear regression performed according to Eq. (21), (22) and (23) are not satisfactory. For all three tested cases, the square of the correlation coefficient R^2 is low (for all diameters it is below 0.20 (Table 2)), which indicates a very poor fit of the simple regression to the experimental data. The calculated value of the t statistic for the b coefficient ($t = 1.4603$; 1.1525; 0.9531) in no case exceeds the critical value $t = 2.262$ for 9 degrees of freedom and at a significance level of 0.05. Therefore, it is not possible to reject the null hypothesis about the insignificance of the slope coefficient Eq. (21), (22) and (23). It was thus demonstrated that there is no effect of yeast size on the rate constant of ultrasonic cell disruption. This is also evidenced by the obtained p values (Table 2), which are greater than the assumed significance level α. The same conclusion can be formulated taking into account the F statistics (Table 2) much smaller than the critical value $F_{0.05,1.9} = 5.12$ at the significance level $\alpha = 0.05$ for 1 degree of freedom in the numerator and 8 degrees of freedom in the denominator. The t-statistic value for the intercept (Table 2) also does not exceed the critical value.

The process of ultrasonic disruption of microorganisms is therefore similar to the disintegration process carried out in a bead mill as a result of only one type of destruction mechanism – axial collision of the beads with the yeast cell. This comes down to the production of transformation volumes $V_{\gamma\zeta}$ in space V, equal to the volume of the destroyed microorganisms. During implosion, a single cavitation bubble disrupts the walls of an adjacent microbial cell, regardless of its size. The process rate constant does not depend on the size of the microorganism. In Fig. 10, 11 and 12, the level of the average value of the constant cell burst rate determined from the $k_{1\zeta}$ values obtained for all size ranges is marked with a red line.

Table 2. Results of multiple regression of the dependence of $k_{1\zeta}$
on D_{min}, D_{mean} and D_{max} ($\alpha = 0.05$).

	D_{min}	D_{mean}	D_{max}
Multiple R	0.4377	0.3586	0.3028
F	2.1325	1.3281	0.9083
df	1.9	1.9	1.9
p	0.1782	0.2788	0.3655
Standard error of estimation	0.0001544	0.0001554	0.0001538
Intercept	0.0002875	0.0003351	0.0003654
Standard error	0.0001840	0.0001732	0.0001661
$t(9) =$	1.5628	1.9247	2.2004
$p <$	0.1525	0.0850	0.0553
beta	0,4377	0.3586	0.3028
Standard error beta	0.2997	0.3112	0.3177
$t(9)$	1.4603	1.1525	0.9531
Average value $k_{1\zeta}$	0.000547	0.000527	0.000517
Standard error $k_{1\zeta}$	0.000136	0.000158	0.000153

4. CONCLUSIONS

The research conducted showed that:

- The process of ultrasonic disintegration of microorganisms is a process of random transformation of dispersed matter.
- The kinetics of cell disruption, both as a whole and in size classes, is well described by a first-order linear differential equation.
- The kinetics of nucleic acid release is very well described by a first-order linear differential equation.
- The cell disruption rate constant $k_{1\zeta}$ does not depend on the cell size.
- The process of ultrasonic homogenization of microorganisms is similar to the process carried out in a theoretical bead mill, in which cells are disrupted only according one mechanism – axial collision of beads with microorganisms.

SYMBOLS

A	light absorbance
C	concentration of nucleic acids released from microbial cells during the process, mg/cm^3
D	diameter, μm
F	sum of the area of relative displacement of objects of set N from the volume safe for them to the transformation volume, m^2
k	process rate constant, 1/s
l	width of the spectrophotometric cuvette, cm

m	number of size classes
M	molar mass, g/M
N	set of material objects
N	number of cells
r	dilution
t	process duration, s
u	average speed of relative displacement of material objects of the set N from the volume safe for them to the transformation volume, m/s
V	volume, m^3
X	degree of disintegration of microorganisms, %
ε	calibration constant, cm^2/M

Subscripts

0	initial value
1	concerns cell disruption
2	concerns the release of nucleic acids
d	concerns disintegrated cells
i	i-th object from the set N
k	final value
max	maximum value
mean	mean value
min	minimum value
α	refers to a volume safe for living microorganisms
β	refers to the volume inaccessible to living microorganisms
γ	refers to the transformation volume
ζ	ζ-th size class

Akcent

–	average value

REFERENCES

Benthin S., Nielsen J., Villadsen J., 1991. A simple and reliable method for the determination of cellular RNA content. *Biotechnol. Tech.*, 5, 39–42. DOI: 10.1007/BF00152753.

Borthwick K.A.J., Coakley W.T., McDonnell M.B., Nowotny H., Benes E., Gröschl M., 2005. Development of a novel compact sonicator for cell disruption. *J. Microbiol. Methods*, 60, 207–216. DOI: 10.1016/j.mimet.2004.09.012.

Chisti Y., Moo-Young M., 1986. Disruption of microbial cells for intracellular products. *Enzyme Microb. Technol.*, 8, 185–204. DOI: 10.1016/0141-0229(86)90087-6.

Chu C.P., Chang B.-V., Liao G.S., Jean D.S., Lee D.J., 2001. Observation on changes in ultrasonically treated waste-activated sludge. *Water Res.*, 35, 1038–1046. DOI: 10.1016/s0043-1354(00)00338-9.

Doulah M.S., 1977. Mechanism of disintegration of biological cells in ultrasonic cavitation. *Biotechnol. Bioeng.*, 19, 649–660. DOI: 10.1002/bit.260190504.

Dumitrașcu L., Lanciu A., Aprodu I., 2022. A preliminary study on using ultrasounds for the valorization of spent brewer's yeast. *The Annals of the University Dunarea de Jos of Galati Fascicle VI – Food Technology*, 46, 141–153. DOI: 10.35219/foodtechnology.2022.2.10.

Geciova J., Bury D., Jelen P., 2002. Methods for disruption of microbial cells for potential use in the dairy industry- a review. *Int. Dairy J.,* 12, 541–553. DOI: 10.1016/S0958-6946(02)00038-9.

Heim A., Solecki M., 1999. Disintegration of microorganisms in bead mill with a multi-disc impeller. *Powder Technol.,* 105, 389-395. DOI: https://doi.org/10.1016/S0032-5910(99)00163-1.

Kacprowicz A., Trawińska A., Solecki M., 2020. Effect of ultrasonic homogenizer geometry on the disintegration of bakery yeast. *Przem. Chem.*, 99, 211–214. DOI: 10.15199/62.2020.2.4.

Middelberg A.P.J., O'Neill B.K., Bogle I.D.L., Snoswell M.A., 1991. A novel technique for the measurement of disruption in high-pressure homogenization: studies on *E. coli* containing recombinant inclusion bodies. *Biotechnol. Bioeng.*, 38, 363–370. DOI: 10.1002/bit.260380406.

Nogueira D.A., da Silveira J.M., Vidal E.M., Ribeiro N.T., Burkert C.A.V., 2018. Cell disruption of *Chaetoceros calcitrans* by microwave and ultrasound in lipid extraction. *Int. J. Chem. Eng.*, 2018, 9508723. DOI: 10.1155/2018/9508723.

Patil M.D., Shinde A.S., Dev M.J., Patel G., Bhilare K.D., Banerjee U.C., 2018. Combined effect of attrition and ultrasound on the disruption of *Pseudomonas putida* for the efficient release of arginine deiminase. *Biotechnol. Progr.,* 34, 1185–1194. DOI: 10.1002/btpr.2664.

Solecki M., 2011. The release of compounds from microbial cells, In: Nakajima H. (Ed.). *Mass transfer – Advanced Aspects*. InTech, Rijeka, 595–618. DOI: 10.5772/21525.

Solecki M., 2013. The theory of random transformation of dispersed matter, In: Nakajima H. (Ed.). *Mass transfer – Advances in sustainable energy and environment oriented numerical modelling*. InTech, Rijeka, 3–30. DOI: 10.5772/52369.

Solecki M., Trawińska A., Kacprowicz A., 2021. The effect of cell size on the kinetics of yeast disintegration in a bead mill. *Powder Technol.*, 380, 584–597. DOI: 10.1016/j.powtec.2020.10.091.

Weber S., Grande P.M., Blank L.M., Klose H., 2022. Insights into cell wall disintegration of *Chlorella vulgaris*. *PLoS One*, 17, e0262500. DOI: 10.1371/journal.pone.0262500.

Yusaf T., 2015. Evaluating the effect of heat transfer on cell disruption in ultrasound processes. *Ann. Microbiol.,* 65, 1447–1456. DOI: 10.1007/s13213-014-0983-z.

Zheng S., Zhang G., Wang H., Long Z., Wei T., Li Q., 2021. Progress in ultrasound-assisted extraction of the value-added products from microorganisms. *World J. Microbiol. Biotechnol.*, 37, 71. DOI: 10.1007/s11274-021-03037-y.

Zielewicz E., 2016. Effects of ultrasonic disintegration of excess sewage sludge. *Appl. Acoust.*, 103, B, 182–189. DOI: 10.1016/j.apacoust.2015.05.007.